PROCEEDINGS OF SCIENCE

The near-infrared broad emission line region of AGN

Hermine Landt*
School of Physics, University of Melbourne, Australia
E-mail: hlandt@unimelb.edu.au

Misty C. Bentz
Department of Physics and Astronomy, Georgia State University, USA
E-mail: bentz@chara.gsu.edu

Bradley M. Peterson
Department of Astronomy, The Ohio State University, USA
E-mail: peterson@astronomy.ohio-state.edu

Martin Elvis
Harvard-Smithsonian Center for Astrophysics, USA
E-mail: elvis@head.cfa.harvard.edu

Martin J. Ward
Department of Physics, University of Durham, UK
E-mail: m.ward@durham.ac.uk

Kirk T. Korista
Department of Physics, Western Michigan University, USA
E-mail: kirk.korista@wmich.edu

Margarita Karovska
Harvard-Smithsonian Center for Astrophysics, USA
E-mail: mkarovska@cfa.harvard.edu

We summarize the main results from our on-going near-infrared (near-IR) and quasi-simultaneous optical spectroscopic programme of broad-emission line AGN. Our near-IR spectra have a large wavelength coverage ($0.8-2.4$ μm), medium resolution and relatively high S/N ratio (>100). The focus is on the the properties of the hot dust component and the kinematics of the hydrogen emitting region. Furthermore, we introduce the near-IR radius-luminosity relationship, which is expected to be used to derive black hole masses in particular of obscured AGN. Roughly a third of our sample are NLSy1s and their properties are compared to those of the total sample.

Narrow-Line Seyfert 1 Galaxies and their place in the Universe - NLS1,
April 04-06, 2011
Milan Italy

*Speaker.

PoS(NLS1)009

1. The observations

We obtained contemporaneous (within two months, during four observing runs) near-IR and optical spectroscopy for a sample of 23 well-known relatively nearby ($z \lesssim 0.3$) and bright ($J \lesssim$ 14 mag) broad-emission line AGN. The observations, which are discussed in detail in [1] and [2], were carried out between 2004 May and 2007 January with a single object being typically observed twice within this period.

The near-IR spectra were obtained with the SpeX spectrograph [3] at the NASA Infrared Telescope Facility (IRTF), a 3 m telescope on Mauna Kea, Hawai'i. We chose the short cross-dispersed mode (SXD, $0.8-2.4$ μm) and a slit of $0.8\times15''$, which resulted in an average spectral resolution of FWHM$\sim$ 400 km s^{-1}. The optical spectra were obtained with the FAST spectrograph [4] at the Tillinghast 1.5 m telescope on Mt. Hopkins, Arizona. We used the 300 l/mm grating and a $3''$ long-slit, resulting in a wavelength coverage of $\sim 3720-7515$ Å and an average spectral resolution of FWHM$\sim$ 330 km s^{-1}. All spectra have a relatively high continuum S/N ratio ($\gtrsim$ 100).

As we discussed in [1], the near-IR broad emission line spectrum of AGN is dominated by a plethora of permitted transitions of mainly hydrogen (the Paschen and Brackett series), helium, oxygen, and calcium, and by the rich spectrum of singly ionised iron. In particular, two of the near-IR Fe II broad emission lines (Fe II 1.05 μm and Fe II 1.11 μm) are observed to be unblended, which means that their measured width can be used to broaden appropriate optical Fe II templates.

2. The hot dust component

Our spectral observations cover the continuum rest-frame frequency range of $\nu \sim 10^{14}-10^{15}$ Hz, which is believed to sample two important AGN emission components, namely, the accretion disc and the hottest part of the putative dusty torus. This special continuum region has been studied so far mainly combining optical spectroscopy with near-IR photometry, with the two frequency ranges usually not observed contemporaneously. Our observations now give us for the first time the opportunity to define the separate continuum components at spectroscopic rather than photometric precision. This permits us to investigate in particular the properties of the hot dust component in greater detail than was possible before.

As we discussed in [2], the study of the spectral shape of the pure AGN continuum requires an adequate subtraction of the underlying host galaxy flux. Then, in the absence of short-term variability, this step should yield an alignment between the AGN optical and near-IR spectral parts. We have estimated the host galaxy contribution in the apertures of both the near-IR and optical spectra using the *Hubble Space Telescope (HST)* images of [5] and [6] and following their approach. For 8/23 objects we did not have suitable *HST* images. In these cases we have estimated the host galaxy contribution based on the linear correlation present between the logarithms of the aperture and the enclosed host galaxy luminosity for the sources with *HST* images. As expected, due to the better seeing achieved in the near-IR and the relatively small extraction aperture used in this band, the host galaxy flux contribution to the near-IR spectra is significantly less than to the optical spectra. Two of our sources (Mrk 590 and NGC 3227) were found to have both near-IR and optical spectra dominated by host galaxy starlight and were excluded from further studies.

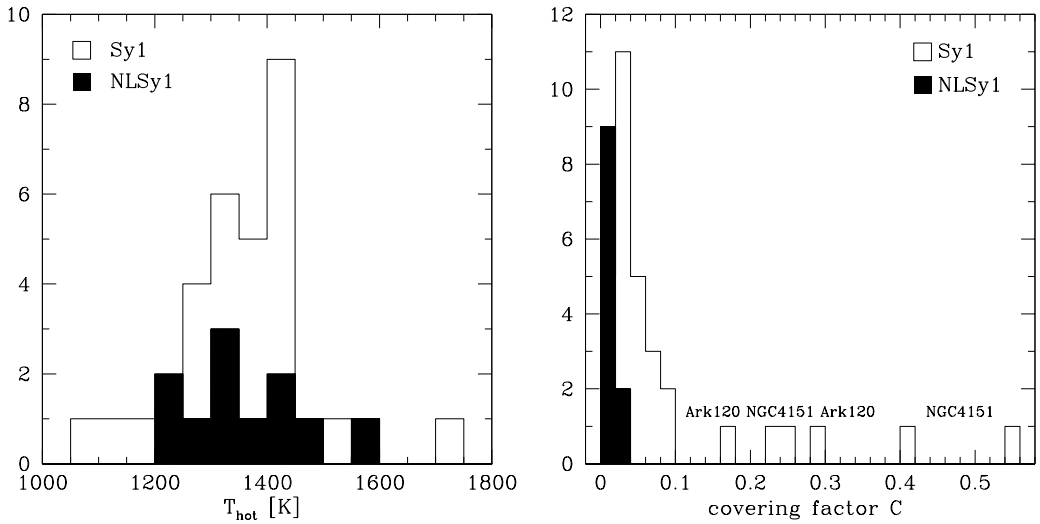

Figure 1: Histograms of the hot dust temperature (left panel) and covering factor (right panel). Whereas the hot dust in NLSy1s (shaded histogram) has a similar average temperature as that of broad-line Sy1s (open histogram), its covering factor in NLSy1s is relatively low, due to the high accretion disc luminosities.

The frequency gap between our near-IR and optical spectra is large enough ($\log \nu \sim 0.05$) that we need to assume an overall spectral shape in order to judge the two parts as being 'aligned'. Therefore, since the AGN continuum blueward of ~ 1 μm is generally thought to be emitted by the accretion disc, we have considered this component as the model and calculated its spectrum for the steady geometrically thin, optically thick case. Assuming an accretion disc spectrum, excess host galaxy contribution to the optical spectrum (but not to the near-IR spectrum) was apparent in the majority of our low redshift ($z \lesssim 0.1$) sources.

The AGN continuum redward of ~ 1 μm is believed to be produced by the hot dust from the putative obscuring torus. Assuming this component is indeed seen in our data, we have subtracted from the total spectrum that of the accretion disc and have fitted to the result a blackbody spectrum. A hot blackbody spectrum appears to approximate well the near-IR AGN continuum in all our sources. In particular, the typical curvature of such a spectrum is evident in our spectra due to their relatively large wavelength coverage. In this respect, we note that the blackbody curvature is not evident in the original spectra (without the accretion disc component subtracted); rather they resemble single power-laws.

The resulting temperatures for the hot blackbody component are in the range of $T_{\rm hot} \sim 1100 - 1700$ K, which are typical values of the dust sublimation temperature for most astrophysical grain compositions. The overall temperature distribution is relatively narrow and has a well-defined mean of $\langle T_{\rm hot} \rangle = 1365 \pm 18$ K. Dividing our sample into NLSy1s (defined to have Paβ broad emission line widths of FWHM$_{\rm Pa\beta} < 2000$ km s^{-1}; 7 sources) and broad-line Sy1s (14 sources), we find that the two object classes have similar mean hot dust blackbody temperatures of $\langle T_{\rm hot} \rangle = 1354 \pm 32$ K and $\langle T_{\rm hot} \rangle = 1369 \pm 22$ K, respectively (Fig. 1, left panel).

The strength of our data set is that it allows us to observe simultaneously the accretion disc and the hot dust emission. Therefore, we can derive for the first time meaningful covering factors for

the dusty obscurer in AGN. If the ultraviolet radiation from the accretion disc emitted into the solid angle, Ω, defined by the dust distribution is completely absorbed and re-emitted in the infrared, the dust covering factor is $C = \Omega/4\pi = \int_{\rm hot} L_\nu d\nu / \int_{\rm acc} L_\nu d\nu \approx 0.4 \cdot (\nu L_{\rm hot}/\nu L_{\rm acc})$, where $\nu L_{\rm hot}$ and $\nu L_{\rm acc}$ are the peak luminosities of the hot blackbody and accretion disc spectrum, respectively. Note that whereas $\nu L_{\rm hot}$ lies only slightly outside the observed spectral range and, therefore, is well-constrained by the data, the accretion disc peak luminosity is strongly model-dependent. We obtain hot dust covering factors in the range of $C \sim 0.01 - 0.6$ and a mean of $\langle C \rangle = 0.07 \pm 0.02$. Considering NLSy1s and broad-line Sy1s separately, we find that the former have a factor of ~ 7 lower average hot dust covering factors than the latter ($\langle C \rangle = 0.013 \pm 0.002$ and $\langle C \rangle = 0.09 \pm 0.02$, respectively; see Fig. 1, right panel).

3. The near-IR virial product and radius-luminosity relationship

The model accretion disc spectrum is fully constrained by the two quantities, mass and accretion rate of the black hole. Two thirds of our sample have black hole masses derived from reverberation mapping campaigns. For the remainder (7 sources) we have estimated this quantity by applying the virial theorem $M_{\rm BH} \propto v^2 r/G$, where v and r are the velocity and radial distance of an orbiting particle, respectively, to the near-IR. Using the width of the Paβ broad component (denoted FWHM$_{\rm Pa\beta}$) as a measure of v and the square-root of the integrated continuum luminosity at 1 μm (denoted $\nu L_{1\mu m}$) as a surrogate for r, we find for the sources with reverberation mapping results that the black hole mass correlates with the near-IR virial product. The observed correlation is $\log M_{\rm BH} = 0.84(2 \log {\rm FWHM}_{\rm Pa\beta} + 0.5 \log \nu L_{1\mu m}) - 16.58$ [2]. The accretion rate can be obtained directly from an approximation of the accretion disc spectrum to the data.

The correlation between black hole mass and near-IR virial product rests strongly on our finding that the accretion disc spectrum, which is believed to be the main source of ionising radiation, extends well into the near-IR and still dominates the AGN continuum at ~ 1 μm. Therefore, a single-epoch near-IR spectrum, ideally obtained through a slit small enough that it excludes most of the host galaxy starlight (see Section 2), can in principle be used to estimate the radius of the broad emission line region. We have recently verified this conjecture [7]. For 14 reverberation-mapped AGN in our sample we have fit a relationship of the form $R \propto \nu L_{1\mu m}^{\alpha}$, where R is the radius of the Hβ broad-emission line region (taken from [6] and [8]). We obtained a best-fit slope of $\alpha \sim 0.5 \pm 0.1$, which is consistent with the slope of the relationship in the optical band [5, 6] and with the value of 0.5 naïvely expected from photoionisation theory. The near-IR radius-luminosity relationship is expected to be relevant particularly for dust-obscured AGN.

4. The kinematics

The profiles of the strongest Paschen lines, Paα and Paβ, are observed to be unblended [1], which makes them well-suited for studies of the geometry and kinematics of the broad emission line region (BELR). A crucial step towards isolating the intrinsic broad-emission line profile is the subtraction of the narrow-emission line component. The narrow-line profile appears inflected, i.e., the transition point between the broad and narrow components is obvious, in roughly half of our sample. Two sources (PG 0844+349 and Ark 120) clearly lack a Paschen narrow-line component,

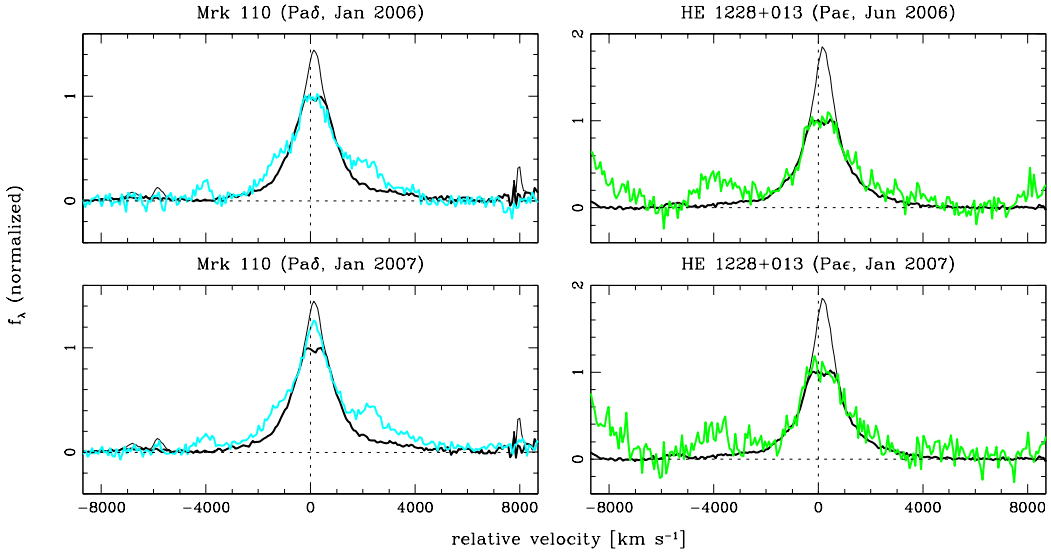

Figure 2: Observed profiles of the Paδ (cyan) and Paε (green) emission lines for Mrk 110 and HE 1228+013, respectively, compared to the template profiles (Paβ and Paα, respectively; black). The disappearing narrow component reveals a flat-topped broad-line profile.

since their profiles have a broad top. However, in the remainder the transition between the broad and narrow components is not perceptible. In [1] we estimated in these cases the contribution of the narrow component to the total profile by fitting to its top part a Gaussian with FWHM equal to that of the narrow emission line [O III] λ5007. This method assumes that the FWHM of [O III] λ5007 is representative of the narrow emission line region (NELR) and subtracts the largest possible flux contribution from this region.

Our method of subtracting the narrow-line contribution in cases where there is a smooth transition between the broad and narrow components yields intrinsic broad-line profiles that are flat-topped. And such flat-topped profiles are the norm in the inflected sources, where the separation between the broad and narrow components is prominent. In support of our method is an effect that we present here for the first time and dub the "disappearing NELR". In all smooth-transition sources we observe that the narrow-line component starts to disappear in the higher-order Paschen emission lines, such as, e.g., Pa9, and in some sources even earlier, e.g., Paδ and Paε in Mrk 110 and HE 1228+013, respectively (see Fig. 2).

If all AGN have flat-topped broad-emission line profiles, the BELR has an outer radius. Assuming that the broad-line gas is virialised and its velocity field is isotropic, we have calculated the BELR outer radius from the width of the flat-top. For this purpose we have used black hole masses from reverberation mapping campaigns and also estimated using the relation we have presented in [2]. In order to test if our method is consistent or if instead it yields widely different results for the smooth-transition and inflected sources, we plot in Fig. 3 (left panel) the radius-luminosity relationship between the BELR outer radius and the integrated luminosity at 1350 Å. We have estimated the latter quantity, which is intimately related to the ionising luminosity, from our accretion disc fits. Both types of sources, and in particular the NLSy1s (red circles), follow the same relationship.

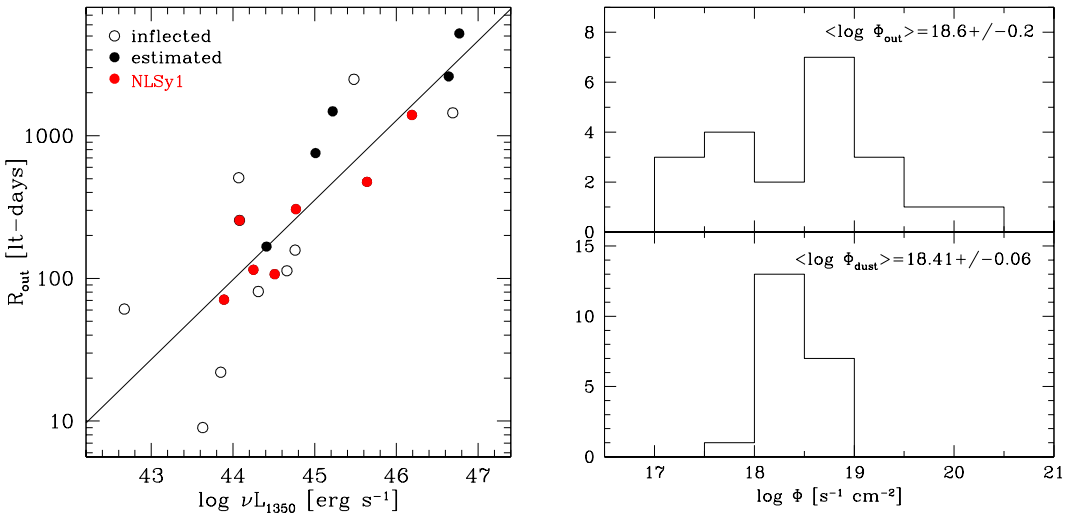

Figure 3: Left: The BELR outer radius versus the integrated luminosity at 1350 Å estimated from accretion disc fits. Open and filled circles indicate sources with an obvious and an estimated transition point between the broad- and narrow-line components, respectively. NLSy1s are highlighted in red. The observed correlation (solid line) has a slope of $\alpha = 0.56 \pm 0.08$. Right: Histograms of the ionising fluxes at the outer radius (upper panel) and at the average hot dust radius (bottom panel). The two distributions have similar means.

A least-squares fit gives a slope of $\alpha = 0.56 \pm 0.08$, consistent with a value of 0.5 expected from photoionisation arguments. Therefore, the BELR seems to cease at a certain ionising *flux*.

We have estimated this BELR limiting ionising flux and show in Fig. 3 (right upper panel) its distribution. We obtain a mean of $\langle \log \Phi_{\rm min} \rangle = 18.6 \pm 0.2$, which is consistent with the range of values that allow for dust sublimation. And in fact, using the hot dust average radii from [2], we obtain a relatively narrow distribution for the ionising flux with a similar mean of $\langle \log \Phi_{\rm hot} \rangle = 18.41 \pm 0.06$ (Fig. 3, right bottom panel). Therefore, it appears that the BELR ceases at that ionising flux which allows dust to sublime, i.e., the BELR is dust-limited.

Already [9] showed that as soon as dust is present the broad-line gas emission diminishes sharply and emission from the NELR is expected at much larger radii. This scenario is well-suited to explain the appearance of the inflected sources with a large gap in velocity field between the BELR and NELR. However, how can the smooth-transition sources fit in this scenario? As Fig. 3 shows, these are mostly high-luminosity sources and appear narrow due to their outer radii being located much further out. The appearance of a prominent velocity gap between the broad and narrow components could then simply be prevented by spectral resolution effects.

References

[1] H. Landt, M. C. Bentz, M. J. Ward, et al.: *The near-infrared broad emission line region of active galactic nuclei I. The observations*, *ApJS* **174** (2008) 282.

[2] H. Landt, M. Elvis, M. J. Ward, et al.: *The near-infrared broad emission line region of active galactic nuclei II. The 1-μm continuum*, *MNRAS* **414** (2011) 218.

[3] J. T. Rayner, D. W. Toomey, P. M. Onaka, et al.: *SpeX: A medium-resolution 0.8-5.5 micron spectrograph and imager for the NASA Infrared Telescope Facility*, *PASP* **115** (2003) 362.

[4] D. Fabricant, P. Cheimets, N. Caldwell, J. Geary: *The FAST spectrograph for the Tillinghast telescope*, *PASP* **110** (1998) 79.

[5] M. C. Bentz, B. M. Peterson, R. W. Pogge, et al.: *The radius-luminosity relationship for active galactic nuclei: the effect of host galaxy starlight on luminosity measurements*, *ApJ* **644** (2006) 133.

[6] M. C. Bentz, B. M. Peterson, H. Netzer, et al.: *The radius-luminosity relationship for active galactic nuclei: the effect of host galaxy starlight on luminosity measurements II. The full sample of reverberation-mapped AGNs*, *ApJ* **697** (2009) 160.

[7] H. Landt, M. C. Bentz, B. M. Peterson, et al.: *The near-infrared radius-luminosity relationship for active galactic nuclei*, *MNRAS* **413** (2011) L106.

[8] K. D. Denney, B. M. Peterson, R. W. Pogge, et al.: *Reverberation mapping measurements of black hole masses in six local Seyfert galaxies*, *ApJ* **721** (2010) 715.

[9] H. Netzer, A. Laor: *Dust in the narrow-line region of active galactic nuclei*, *ApJ* **404** (1993) 51.